Visualization and measurement of quantum rotational dynamics

R. M. Dimeo[a)]
NIST Center for Neutron Research, National Institute of Standards and Technology, 100 Bureau Drive, Gaithersburg, Maryland 20899

(Received 30 July 2002; accepted 14 November 2002)

An introduction to quantum rotational tunneling and libration is presented with an emphasis on obtaining a qualitative understanding of this phenomenon through visualization of the dynamics, simple approximations, and measurements. The tunneling and librational dynamics of small molecular rotors are discussed using a very simple model of the rotational potential. Numerical calculations of the evolution of probability packets are carried out for the low-lying states and the connection is made between the quantum and classical librational dynamics. Finally, we present measurements of these quantum rotations using inelastic neutron scattering and show in particular how neutron scattering measurements of the ground state tunnel splitting and first librational transition can be used to characterize the magnitude and shape of the potential hindering the motion of the rotor. Some conceptual and computational problems are included that are suitable for undergraduate students.
[DOI: 10.1119/1.1538575]

I. INTRODUCTION

Studying the quantum rotational dynamics of molecular systems can provide detailed information on the forces between molecules (intermolecular interactions) and between the molecular constituents within a single molecule (intramolecular interactions). It is not surprising then that rotational spectroscopy has been widely used as a means to characterize these interactions.[1] Obtaining an understanding of the rotational dynamics requires one to have a physically reasonable model of the molecular system. In general, however, a microscopic description of the rotational dynamics of a molecular system can be quite complicated. For molecules of even modest complexity there can be many sub-units undergoing simultaneous rotation + translation thus requiring multiple coordinate systems for a detailed analysis. A simple three-dimensional rotor such as solid hydrogen (H_2) is essentially a free spherical rigid rotor and its rotational dynamics have been studied extensively.[2] The rotational motion of a tetrahedral molecule such as methane (CH_4) is somewhat more difficult to analyze but the dynamics of the molecular solid are still tractable.[3]

Arguably the simplest type of rigid rotors are those that have a single rotational degree of freedom such as the methyl halides containing methyl groups (CH_3) or the ammonia compounds (containing ammonia groups, NH_3). In these molecular solids, the methyl or ammonia groups can rotate about a fixed molecular axis, under the influence of a crystal field (an orientational potential) hindering rotation, thus displaying a variety of different rotational motions. The types of motions that can be observed are libration, stochastic reorientation, and quantum rotational tunneling. Libration is the quantum analog of classical torsional oscillation in which the CH_3 group (for instance) oscillates within the hindering potential. Stochastic reorientation is a rotational motion in which thermal fluctuations in the crystal provide enough energy to overcome the hindering barrier, thus enabling spontaneous reorientation of the CH_3.

Quantum rotational tunneling is somewhat more difficult to understand because it has no classical analog. Translational tunneling is better known and has been discussed at length.[4–13] Pauling recognized in 1930 that molecular crystals such as hydrogen can exhibit quantized rotational motion including rotational tunneling.[14,15] Rotational tunneling is a phenomenon whereby a molecule (or a molecular sub-unit) whose rotational motion is hindered by an orientational barrier, reorients itself via tunneling through the barrier. Since the 1930s, rotational tunneling has been observed in many molecular systems from solids to gases.[3,16] In rotational tunneling the ''particle'' that tunnels can be a molecular subgroup such as a methylene group (CH_2), a CH_3 group, or even an entire molecule such as H_2 or CH_4. The description of the coherent motion of the constituent atoms is called the single particle model. The single particle motion is determined by the molecular environment. If there is no molecular field that hinders the single particle motion, then the rotor undergoes quantized free rotation. If the motion of the single particle is hindered, a situation that we will consider, then the quantum rotations can include rotational tunneling and librations.[3,16]

The related problem of quantum rotations in pendula where the potential, $V(\theta)=V_0(1-\cos\theta)$ for $V_0=mgl$, has only a single minimum rendering tunneling impossible.[17–21] Nevertheless, the quantum pendulum provides a useful example of torsional oscillations in the limit of large V_0 and free quantum rotations in the limit of small values of V_0.[21] Recent experimental illustrations of free rotations in ethane (containing CH_3 groups) and torsional oscillations of potassium hexachloroplatinate (with a $PtCl^-$ group) have been discussed in this context of quantum pendula.[21]

In the same way that the Josephson junction, scanning tunneling microscope, and the tunnel diode exploit translational tunneling, rotational tunneling spectroscopy has found a practical use, namely the identification and refinement of atom—atom potentials. Recently the method of rotational tunneling spectroscopy has been used in conjunction with crystallographic measurements and molecular mechanics methods to provide a comprehensive set of techniques for the microscopic characterization of molecular solids.[22] The subject of quantum rotational tunneling, although straightforward, has not appeared in this journal to our knowledge. However, the level of physics and mathematics necessary for

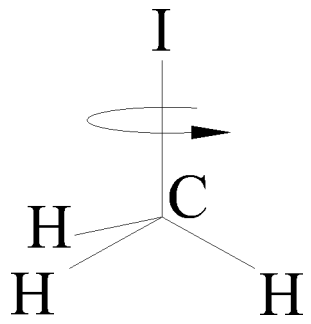

Fig. 1. Stick diagram of methyl iodide, CH_3I. Rotations considered in this paper are shown with the arrow.

an understanding is at an advanced undergraduate level, and we illustrate the main features of rotational tunneling visually. In this paper we discuss the tunneling and librational dynamics of CH_3 groups within the single particle model and illustrate how measurements of tunneling and libration can be used to extract detailed information on the local molecular environment.

This paper is organized as follows. In Sec. II we review the problem of hindered rotation for CH_3 groups and discuss the different types of motion possible. Section III contains a brief review of neutron scattering, particularly from CH_3 groups, and measurements from CH_3I are presented and discussed. Section IV contains a number of conceptual and computational problems suitable for advanced undergraduate students.

II. METHYL GROUP DYNAMICS

The single particle model often can be used to describe the dynamics of solids composed of molecules with at least one methyl group. A methyl group is best described as a pyramid composed of three hydrogen atoms at the base and a carbon atom at the apex with an H–H distance $d_{\mathrm{HH}} \simeq 1.78$ Å. One particular small molecule, methyl iodide (CH_3I), contains a single methyl group and is shown in Fig. 1. The moment of inertia about the C atom perpendicular to the plane of the H atoms is $5.3\times10^{-47}\,\mathrm{kg\,m^2}$, which sets the energy scale for the quantum rotational dynamics. Unhindered rotations of the CH_3 group can be described in terms of the Schrödinger equation,

$$-\frac{\hbar^2}{2I}\frac{d^2}{d\theta^2}\psi_n(\theta)=E_n\psi_n(\theta), \tag{1}$$

where θ is the coordinate specifying the angular orientation of the CH_3 group. The free rotor wave functions (see Appendix A) form a complete basis set for Eq. (1) and can be used to obtain the energy levels, $E_j=Bj^2$, where $B=\hbar^2/2I=654\,\mu\mathrm{eV}$ and j is the rotational quantum number.

The motion of the CH_3 group sub-unit can be described in terms of a potential composed of an intramolecular term and an intermolecular term. In the gas phase the intramolecular term dominates whereas the intermolecular term is dominant in the dense solid phase. We restrict our discussion in this paper to the low temperature solid phase and hence only consider the intermolecular potential. This term can be decomposed into an attractive van der Waal's term, a term due to steric (short-range) repulsion, and other electrostatic multipole forces.[23] A calculation of the overall contribution to the intermolecular potential of each of these terms can be performed for a molecular solid whose structure is known and can often result in a simplification where the total potential is replaced by a term encapsulating the symmetry of the rotating group and a term encapsulating the symmetry of the local environment. In this view the threefold symmetry of the CH_3 group constrains the symmetry of the total intermolecular potential to be at least threefold. Thus the potential can be expanded in a Fourier series in multiples of 3θ,

$$V(\theta)=\sum_{m=0}^{\infty} v_{3m}\cos(3m\theta+\alpha_m). \tag{2}$$

If the local molecular environment has no symmetry then the first two terms ($m=0,1$) provide an adequate description of the dynamics and the phase factors, α_0 and α_1, can be set to zero without loss of generality.[16] Then the full Hamiltonian can be expressed as

$$H=-\frac{\hbar^2}{2I}\frac{d^2}{d\theta^2}+\frac{V_3}{2}(1-\cos 3\theta). \tag{3}$$

This is the Mathieu equation whose solution has been presented in this journal.[21] This Hamiltonian can be solved numerically for a particular value of the barrier height, V_3, as discussed in Appendix A. The solution over a broad range of barrier heights is shown in Fig. 2. As a reference, the dashed lines in Fig. 2 indicate the barrier heights for two systems, sodium acetate trihydrate ($CH_3COONa\cdot 3H_2O$) and CH_3I. There are two limits for the motion shown in Fig. 2. In the limit of high barrier, small deviations from one of the three equilibrium positions results in nearly harmonic motion with the usual quantized energy levels,

$$E_n=(n_{\mathrm{lib}}+\tfrac{1}{2})\hbar\omega_0, \tag{4}$$

where the oscillation frequency is given by

$$\omega_0=3\sqrt{\frac{V_3}{2I}}, \tag{5}$$

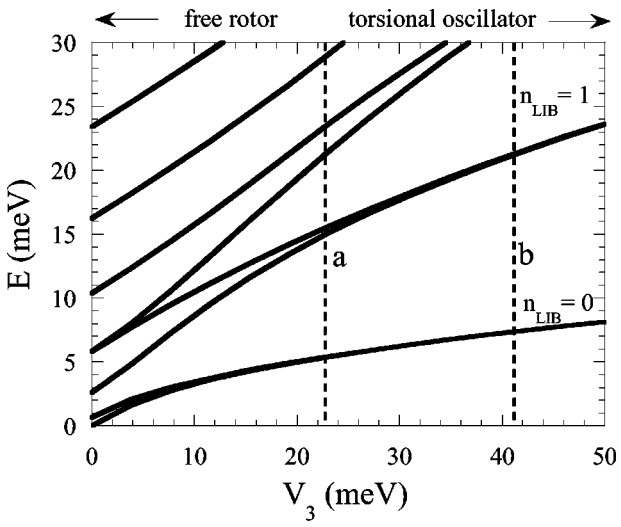

Fig. 2. Eigenvalues for a CH_3 group as a function of the barrier height, V_3. The dashed line labeled a corresponds to the barrier for sodium acetate trihydrate and b corresponds to methyl iodide. The first two librational levels are labeled by the quantum number n_{lib}.

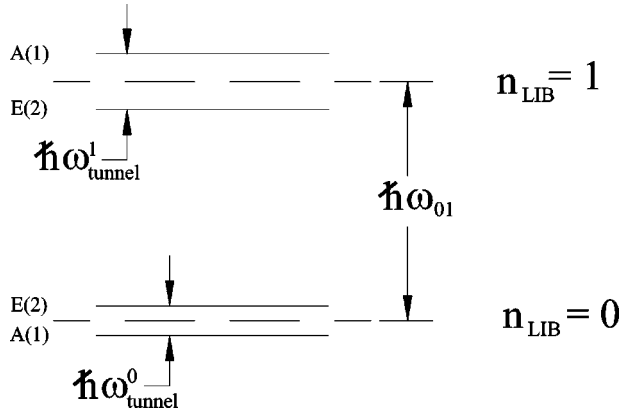

Fig. 3. Schematic illustration of the first two librational levels as intercepted by one of the dashed lines in Fig. 2. The symmetries of the eigenstates are denoted by labels A and E and the degeneracy of the states is given in parentheses.

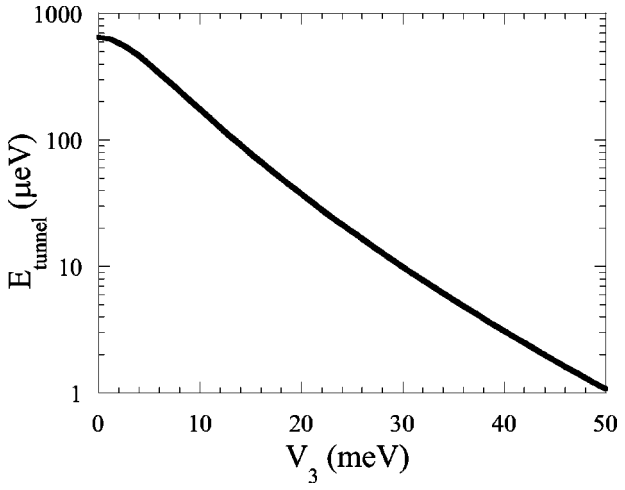

Fig. 4. Tunnel splitting of the ground librational state. The approximate exponential dependence of the tunnel splitting on the barrier height is clearly seen.

and I is the moment of inertia.[21] The librational transitions (the energy difference between the librational levels) in this limit are approximately constant, given by $\hbar\omega_0$. In the limit of low barrier, the energy levels are approximately the free rotation levels discussed previously with transitions given by $\Delta E_j = E_j - E_{j-1} = (2j-1)B$ for $j=1,2,3,\ldots$.

In the intermediate regime where the barrier is not too high or too low, we can understand the rotational dynamics from the simplified energy-level diagram shown in Fig. 3. In this figure, which emphasizes the eigenvalues intersected by one of the dashed lines in Fig. 2, we have exaggerated the spacing between the levels. The lowest two librational levels, $n_{\text{lib}}=0$ and 1, are shown as well as their tunnel split sublevels. The transition from the ground state ($n_{\text{lib}}=0$) to the first excited librational state ($n_{\text{lib}}=1$), denoted by $\hbar\omega_{01}$, can differ from the ground state tunnel splitting ($\hbar\omega^0_{\text{tunnel}}$) by several orders of magnitude. This large difference in the librational and tunneling transitions is an important practical point to consider in measurements of rotational tunneling. Effectively this means that, at low temperature where the thermal population of the excited librational states is negligible, the system can be approximated by a two-state model.

We note also that the invariance of the Hamiltonian (3) under rotations of $2\pi/3$ causes a degeneracy in the tunnel-split librational states. In the language of group theory, solutions of H in Eq. (3) belong to the C_3 point group which possesses two symmetry species.[24] These species, designated A (a singlet), which is symmetric and E (a doublet), which is antisymmetric, are labeled accordingly in Fig. 3. The symmetry of the rotational wave function has a profound effect on the overall molecular wave function and its influence will be discussed in Sec. III.

The rotational excitations observed in measurements involve transitions between the eigenvalues shown in Fig. 2. Measurement techniques such as nuclear magnetic resonance (NMR) and neutron scattering (discussed in Sec. III) probe these transitions directly by the transfer of precisely the amount of energy by which the eigenvalues differ. The tunneling transition, also called the tunnel splitting of the librational ground state, is shown in Fig. 4 as a function of barrier height. Clearly, the Bohr frequency corresponding to the tunneling energy decreases as the barrier increases. This behavior is due to the fact that the wave functions tend to overlap less for larger barriers. Thus the frequency of the tunneling events diminishes. Perhaps the most important characteristic of Fig. 4 is the apparent exponential dependence of the tunnel energy on barrier height, V_3. The sensitivity of the tunnel energy on barrier height can be exploited to probe the magnitude of the barrier.

The barrier height dependence of the first librational transition calculated from a numerical diagonalization of the Hamiltonian in Eq. (3) using the harmonic approximation is shown in Fig. 5. The first librational transition is simply the difference between the average of the lowest two and the following two eigenvalues in the limit of high barriers. We expect the harmonic approximation for the librational frequency, Eq. (5), to improve as the barrier height increases. However, Fig. 5 clearly shows that when $V_3/B \gg 1$, the slopes of the curves agree, but the harmonic approximation systematically overestimates the actual value. In fact the agreement improves with increasing barrier height but the convergence is quite slow. It can be shown (see Appendix B)

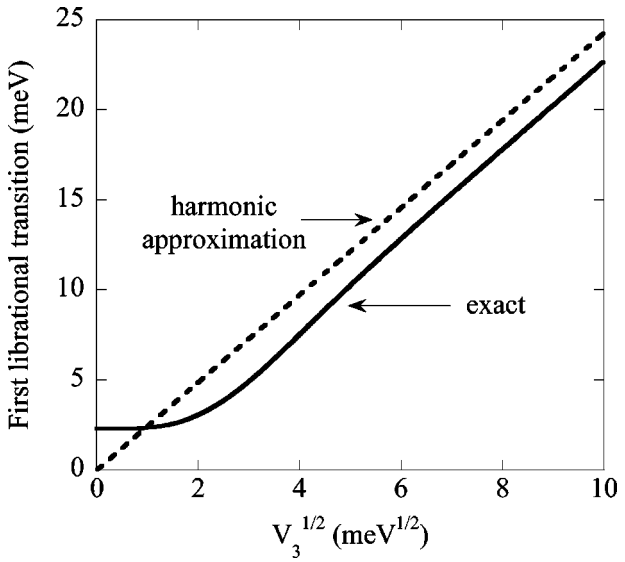

Fig. 5. Barrier height dependence of the first librational transition (solid line). The dashed line is the harmonic approximation, $\hbar\omega_0$.

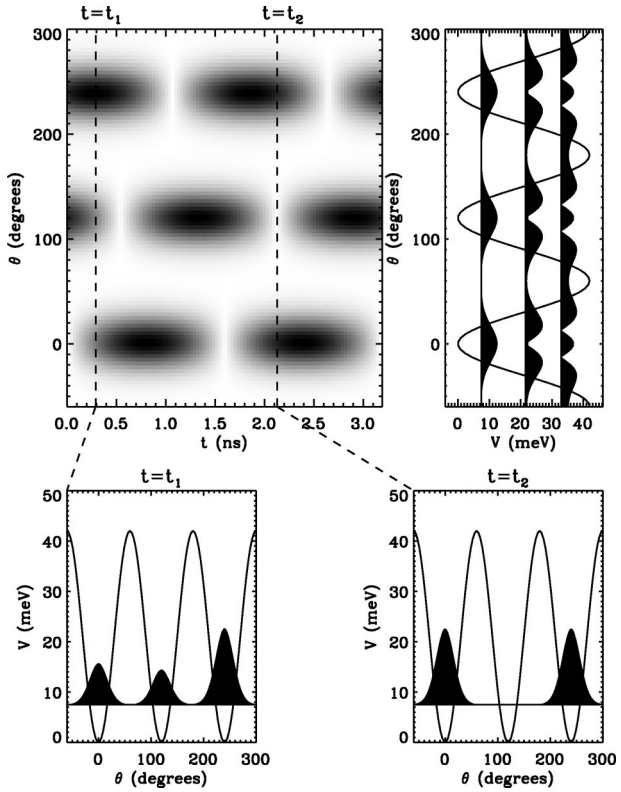

Fig. 6. Time evolution of the probability density when transitions are induced between the two levels in the tunnel split librational ground state. The upper right-hand panel shows the potential barrier for $V_3=42$ meV and the probability densities for the lowest three stationary librational states for reference. The bottom panels show the probability densities at two points in time, $t_1=0.3$ ns and $t_2=2.1$ ns.

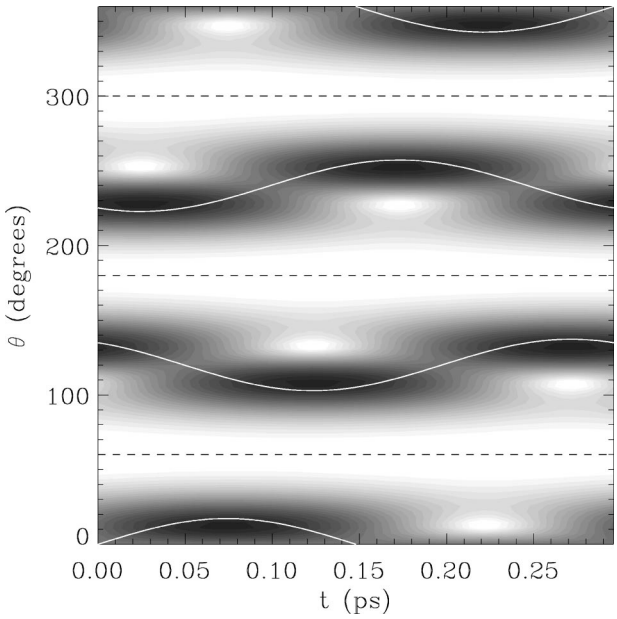

Fig. 7. Evolution of the probability density when transitions are induced between the ground librational state and first excited librational state, $\hbar\omega_{01}$. The probability density sloshes back and forth periodically within each potential minimum. The white solid lines are given by Eq. (10) indicating the classical oscillatory equation of motion. Note the difference in time scale compared with Fig. 6.

that the classical turning point decreases only as $V_3^{-1/4}$, and thus the small angle approximation is approached very gradually.

We can calculate the dynamics of the tunneling and libration processes using the eigenfunctions and eigenvalues found through the numerical diagonalization procedure. As will be described in Sec. III, a neutron is capable of inducing a transition between the rotational eigenstates. In general the process can be described by

$$P(\theta,t)=|\psi(\theta,t)|^2, \tag{6}$$

which is the probability of finding the methyl group oriented at an angle θ (with respect to some arbitrary direction) at time t (with respect to some arbitrary origin in time). In Eq. (6) ψ is represented as a sum over the eigenstates, $\langle\theta|n\rangle$, of the Hamiltonian, Eq. (3), as

$$\psi(\theta,t)=\sum_{n=1}^{\infty} a_n \exp(-iE_n t/\hbar)\langle\theta|n\rangle, \tag{7}$$

where

$$a_n=\int_0^{2\pi} d\theta\,\psi(\theta,0)\langle\theta|n\rangle. \tag{8}$$

Note that in Eqs. (6) and (7) n denotes the (possibly degenerate) eigenstates. For simplicity, we will assume that the neutron couples the lowest two eigenstates of the Hamiltonian, Eq. (3). The results of such a coupling are shown for $V/B=63$ in Fig. 6. It is clear that the region of largest probability density oscillates in time among the three potential minima, whereas the region of least probability is at the maxima of the potential.

The librational dynamics can be illustrated similarly except that now we assume that the neutron couples the ground librational state and the first excited librational state. The result is shown in Fig. 7. We can see that the probability density ''sloshes'' back and forth within each of the potential minima. This type of motion is consistent with the classical notion of libration in which the librating particle oscillates in space. This behavior, a consequence of Ehrenfest's theorem, is similar to the behavior of a Gaussian wave packet in an harmonic potential where the expectation values of the momentum and position operators follow classical trajectories.[25,26] In fact the classical probability density for the librating system is given by

$$P_{\rm cl}[\theta(t)]=\delta[\theta(t)-\theta_{\rm cl}(t)], \tag{9}$$

where $\theta_{\rm cl}(t)$ can be written as

$$\theta_{\rm cl}(t)=\theta_{\rm tp}\sin(\omega t+\alpha). \tag{10}$$

The classical turning point, $\theta_{\rm tp}$, is given by

$$\theta_{\rm tp}=\frac{1}{3}\cos^{-1}\left(1-\frac{\hbar\omega}{V_3}\right), \tag{11}$$

and α is the phase shift and $\omega=\omega_{01}$ is the frequency difference ω between the librational levels. Equation (10) is superposed on Fig. 7 to show the correspondence between the quantum and classical librational motion.

The evolution of the excited state tunneling process, $\hbar\omega^1_{\rm tunnel}$, is shown in Fig. 8. The similarity with Fig. 6 is obvious and the main difference is the appearance of a node in the center of each well. The time-development of the librational transition, $n_{\rm lib}=1\rightarrow 2$ or $\hbar\omega_{12}$, is shown in Fig. 9.

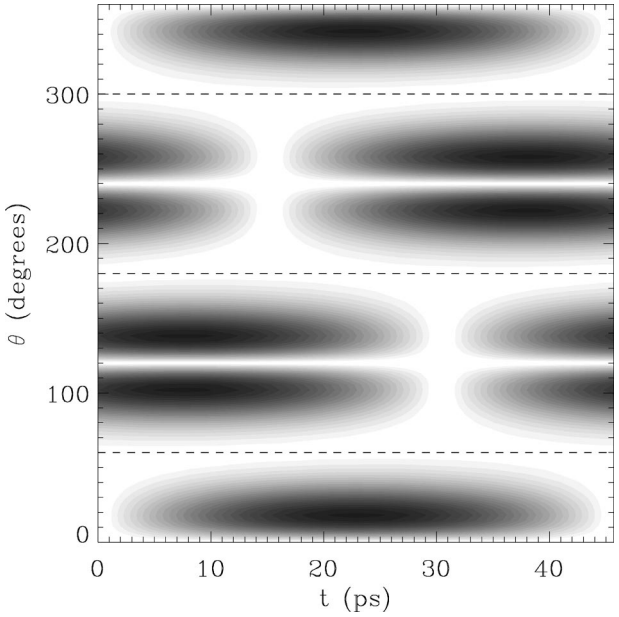

Fig. 8. Same as Fig. 6 but for the transition induced between the two levels of the tunnel split first excited librational state, $\hbar\omega^{1}_{\text{tunnel}}$.

Again we can immediately see the similarity to the transition $\hbar\omega_{01}$ in Fig. 7. The classical trajectory, Eq. (10), based on the excited state classical turning point and librational frequency, $\omega=\omega_{12}$, has also been superposed to illustrate the semi-classical nature of the motion. In both cases involving transitions between (or within) the higher librational eigenstates, the increase in the kinetic energy is made manifest by the increased ''wiggliness'' of the probability density. In still higher excited states, differences in the amount of ''wiggliness'' can be seen in different regions of the potential well, thus illustrating the ''wiggliness'' as a local measure of the kinetic energy.[27,28]

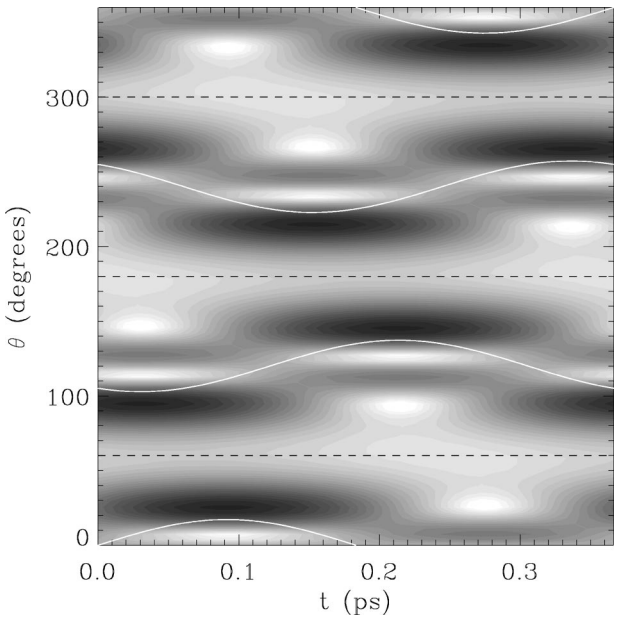

Fig. 9. Same as Fig. 7 except for the transition induced between the first and second excited librational states, $\hbar\omega_{12}$.

III. MEASUREMENTS OF ROTATIONAL TUNNELING

The hindered motions of a CH_3 group discussed in Sec. II can be measured using a number of techniques including NMR, neutron scattering, heat capacity, microwave spectroscopy, optical spectroscopy, infrared spectroscopy, and other techniques.[16] Microwave spectroscopy is typically used for systems in the gas phase where one seeks information about the intramolecular interactions rather than intermolecular interactions.[1] In general, light scattering techniques cannot be used to measure quantum rotational tunneling of CH_3 groups because such rotations involve a change in the nuclear spin state of the molecular wave function. Such changes, which require coupling to the nuclear spin, can be induced using NMR, via dipole–dipole coupling, and neutron scattering. The neutron, possessing nuclear spin $\hbar/2$, couples directly to the nucleus of the scatterer via the nucleon–nucleon interaction. The short-range neutron–nucleon interaction for low-energy neutrons can be treated in the first Born approximation, thus making the interpretation of the scattering data relatively straightforward. In a very simple view, rotational spectra measured with neutron scattering provide direct information on the energy levels of the scattering system.

To appreciate the utility of neutron scattering in measuring quantum rotations, we must first clarify the notion of rotational tunneling from the point of view of the rotor's constituents. For our purposes the hydrogen atoms in the CH_3 group can be viewed as protons. If we imagine a CH_3 group with a well-defined orientation such that we have labeled protons on labeled sites, then we can identify a particular orientation of the CH_3 group by the proton location such as $|123\rangle$. The successive state of a 120° reorientation of the molecule via tunneling is then represented as $|312\rangle$. These states are often referred to as ''pocket states,'' because they correspond to wave functions that are highly localized in the minima of the potential well, that is, in the ''pockets.''[3,16] The tunneling dynamics evolve according to $|123\rangle\rightarrow|312\rangle\rightarrow|231\rangle$ with the Bohr frequency given by $E_{\text{tunnel}}/\text{h}$.

Section II alluded to the fact that the symmetry of the rotational wave functions, the solutions to (3), has a profound influence on the overall molecular wave function. In fact, the nature of a quantum rotation is directly related to the symmetry of the wave function. In order to understand this, we must examine the components of Ψ_{mol}, the molecular wave function. In the Born–Oppenheimer approximation the molecular wave function can be decomposed as $\Psi_{\text{mol}}=\psi_{\text{trans}}\psi_{\text{el}}\psi_{\text{vib}}\psi_{\text{rot}}\psi_{\text{ns}}$, which are the translational, electronic, vibrational, rotational, and nuclear spin functions, respectively.[29] In order to induce a quantum rotation of the CH_3 group, a change in the nuclear spin state must occur. At low temperature we can assume that Ψ_{mol} is in the ground electronic state. A quantum rotation of a CH_3 group is a symmetry operation and thus it is equivalent to a cyclic permutation of the nuclei. Permutation of the nuclei leave the translational and vibrational parts of the molecular wave function unchanged so that we may ignore these terms. Therefore the only portions of Ψ_{mol} relevant to rotational motion are the rotational and nuclear spin wave functions.

Because the CH_3 group is composed of three (indistinguishable) fermions, Ψ_{mol} must be antisymmetric under exchange of any two protons. Therefore, the rotational wave

function must be of the symmetric A species when the nuclear spin wave function is antisymmetric.[3,16,30] Therefore the allowed combinations of the molecular wave function are

$$\Psi_{\mathrm{mol}} = \psi_{\mathrm{rot}}^{\mathrm{E}} \psi_{\mathrm{ns}}^{\mathrm{A}} \psi_{\mathrm{trans}} \psi_{\mathrm{el}} \psi_{\mathrm{vib}}, \tag{12}$$

and

$$\Psi_{\mathrm{mol}} = \psi_{\mathrm{rot}}^{\mathrm{A}} \psi_{\mathrm{ns}}^{\mathrm{E}} \psi_{\mathrm{trans}} \psi_{\mathrm{el}} \psi_{\mathrm{vib}}. \tag{13}$$

Equations (12) and (13) state that, in order to keep the overall antisymmetry of the molecular wave function, a change in the rotational state requires a change in the nuclear spin. In a neutron scattering experiment, the neutron couples directly to the nuclear spin of the target and can change the spin state.

As mentioned in Sec. II, the two-state model can be used as an approximate description of the methyl dynamics. Therefore one might consider using heat capacity to observe the Schottky anomaly[31] associated with the energy difference, $\hbar\omega_{\mathrm{tunnel}}^{0}$, of the two states. This method has been successful in measurements of one particular tunnel splitting in CH_4 where phonons induce the transition,[32] a phenomenon known as spin conversion. However, the heat capacity of nitromethane (CH_3NO_2) showed no evidence for the tunneling transition.[33] Neutron scattering measurements, though, revealed a tunneling excitation at 34 μeV.[34,35] The disagreement between the measurements was appreciated by the researchers who performed the calorimetric measurements as they pointed out ''it is thus possible for neutron scattering and calorimetric measurements to yield apparently contradictory views of an array of tunneling states.''[33] The origin of the different results comes from the nature of the two measurement processes. In the calorimetric measurements, there is no mechanism that can induce a change in the nuclear spin state that can subsequently induce the necessary change in the rotational state. Contrary to the heat capacity measurement of CH_3NO_2 where phonons induce a transition between states of the same symmetry, phonons cannot induce a transition between states of different symmetry. As discussed in the previous paragraph, the tunnel split states for methyl rotors have different symmetry (see Fig. 3), so they require a change in the nuclear spin state which is not possible with phonons. Thus neutron scattering allows direct observation of the tunneling excitations regardless of the symmetry of the states.

In an inelastic neutron scattering measurement the incident neutron can impart both energy (E) and momentum (**p**) to the scattering system.[36] Cold neutrons refer to those whose de Broglie wavelength ($\lambda = h/p$) is on the order of 4–10 Å, and energies in the range of 0.1–5 meV. The variation of scattering intensity with momentum transfer provides information on the geometry of the motion and the variation with energy transfer provides information on the eigenstates of the system. The combination of geometrical and dynamical information make neutron scattering uniquely suited as a probe of molecular dynamics.

The geometry of the scattering process is illustrated in Fig. 10. The incident neutron has an energy E_i and a momentum $\mathbf{p}_i = \hbar\mathbf{Q}_i$, where $\mathbf{Q}_i$ denotes the wave vector of the incident neutron. The magnitude of the wave vector is related to the wavelength via $Q_i = 2\pi/\lambda_i$, so that the dimension of Q is inverse length and the popular units used are Å^{-1}. Similarly, the energy and momentum of the scattered neutron are given by E_f and $\mathbf{p}_f = \hbar\mathbf{Q}_f$, respectively. Thus the energy transfer and magnitude of the momentum transfer are given by $E = E_i - E_f$ and $p^2 = p_i^2 + p_f^2 - 2p_i p_f \cos\theta$. Neutron spectrometers typically can measure molecular dynamics in the energy (time) range from less than μeV (ns) to meV (ps).

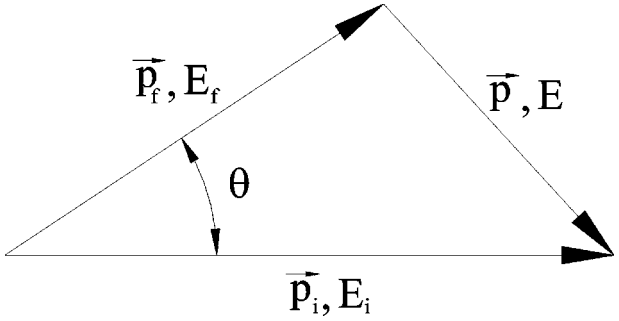

Fig. 10. Geometry of an inelastic neutron scattering experiment.

Usually one measures rotational tunneling below 50 K. As the temperature increases, phonons with an energy comparable to the librational transition energy, $\hbar\omega_{01}$, modulate the potential barrier thus destroying the coherence of the tunneling motion of the rotor.[37,38] Because the librational levels are so far apart ($\sim O$ (10 meV)), thermal population of the higher librational states does not become appreciable at low temperature. Because the tunnel-split librational ground state energy is much lower in magnitude than the first excited state, the effects of the higher excited states on the ground state can safely be ignored at low temperatures.

The scattered intensity of CH_3I for very low energy transfers collected over a wave vector transfer spanning 0.62 to 1.68 Å^{-1} is displayed in Fig. 11. These measurements were performed at the NIST Center for Neutron Research (NCNR) using a technique known as neutron backscattering spectroscopy.[39] There are three prominent features in the spectrum. The large scattering intensity centered on $E = 0$ is the elastic peak and is due to scattering from molecules that either do not move on the time scale of the instrument or whose original orientation is identical to its final orientation. The two satellite peaks located around $\pm 2.4\ \mu$eV are peaks

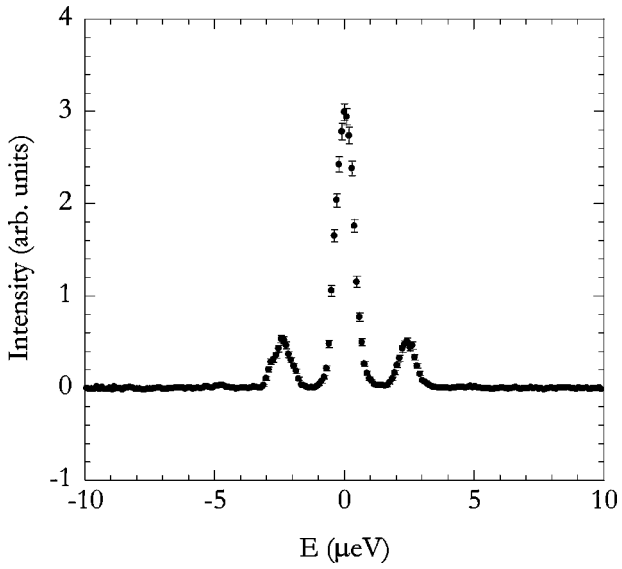

Fig. 11. Neutron scattering data for mi at 10 K. Satellite peaks arise from transitions within the tunnel-split ground librational state.

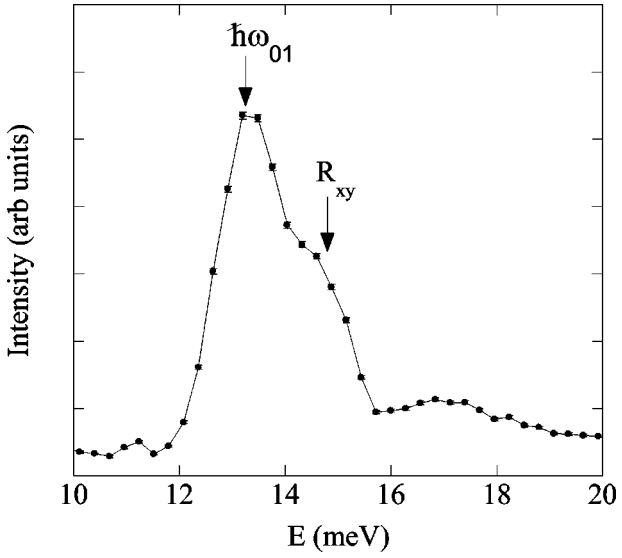

Fig. 12. Neutron scattering data for mi at 10 K. The two dominant features are the $0\rightarrow1$ librational transition ($\hbar\omega_{01}$) and a rotation of the molecule about an axis perpendicular to the main molecular axis (R_{xy}).

arising from the tunnel split librational ground state. The interpretation of this inelastic spectrum is straightforward. The incident neutron has approximately equal probability of gaining or losing 2.4 μeV, thus causing a transition between the E and A states ($\hbar\omega^{0}_{\text{tunnel}}$) in the ground librational state ($n_{\text{lib}}=0$). Note that the measurements here were taken at a temperature low enough that the excited states were largely unpopulated. Thus the shape of each of the peaks is determined by the resolution of the instrument.

An inelastic neutron scattering measurement of the lowest librational transition, $\hbar\omega_{01}$, is shown in Fig. 12. The measurements shown here were carried out using a filter-analyzer neutron spectrometer.[40] In this technique, only neutrons that lose energy are detected. This means that the neutron can create a librational excitation. Unfortunately, measurements at these larger energy transfers are not as straightforward to interpret as the tunneling measurements. The main reason for the difficulty is that there are many different types of excitations that the incident neutron can create whose energies are of the same order as the librational transitions. The data shown in Fig. 12 clearly show at least two peaks whose centers are very close together. Disentangling the origin of the peaks can be aided by deuterating the methyl groups (CH_3 becomes CD_3). The deuteration increases the moment of inertia by a factor of 2 and reduces the librational transition by a factor of $\sqrt{2}$ [see Eq. (5)]. Indeed such measurements were performed resulting in a clear separation of the two peaks with the lower energy peak decreased by $\sqrt{2}$.[41] Thus the lower energy peak is assigned as the $\hbar\omega_{01}$ transition. The value of the transition based on a fit of a Gaussian to the data is 13.4 meV. In a similar type of analysis, the higher energy component in the figure is assigned to rotations (R_{xy}) of the molecule about an axis perpendicular to the main molecular axis.

The values for the tunneling energy and librational transition energy can be used to determine the validity of the model Hamiltonian, Eq. (3), and to extract the barrier height, V_3. As discussed in Appendix A, numerical diagonalization of the Hamiltonian is used to determine the tunneling and librational energies for a particular barrier height. The tunneling energy, 2.43 μeV, corresponds to a barrier height of $V_3=42.2$ meV. The librational transition corresponding to $V_3=42.2$ meV is 14.0 meV. Conversely, a librational transition of 13.4 meV corresponds to a barrier height of 39.0 meV and a tunneling energy of 3.5 μeV. These differences in the resulting tunnel splitting illustrate the sensitivity of the tunneling energy to changes in the barrier height. We select the first value, 42.2 meV, for the barrier because the tunneling is so much more sensitive to the barrier than the librational transition. Thus our measurement of the librational transition, $\hbar\omega_{01}=13.4$ meV is close but too low by a margin larger than the uncertainty in the measurement. The discrepancy could come from a number of sources. First, the truncation of the Fourier series for the potential, Eq. (2), at the first two terms may be premature. In fact, the measurements by Prager and co-workers[41] were analyzed using an additional small sixfold term in the potential energy function. Another source of the disagreement could be a coupling between the rotations of the methyl group about the main molecular axis and the perpendicular axis (R_{xy}) not accounted for in the potential. Such discrepancies could be explained via a calculation of the *true* potential barrier via a molecular mechanics calculation in which the potential is calculated based on the low temperature solid structure and the correct interactions between the atoms.

IV. PROBLEMS FOR FURTHER DISCUSSION

(1) For a molecular gas, why does the intramolecular potential term generally dominate the total potential of the system?

(2) For an n-fold symmetric barrier, $V(\theta)=(V_n/2)(1-\cos n\theta)$, calculate the approximate frequency of the ground librational state. Make sure that you recover Eq. (5) for $n=3$.

(3) For the n-fold symmetric barrier considered in the previous problem, how many sub-states comprise the ground librational state?

(4) Describe a suitable set of basis functions in which one could expand the Hamiltonian (3) so that convergence to the exact eigenvalues would be rapid in the limit of high barriers.

(5) In the limit of small barrier height, what do you expect the ''tunneling'' plot shown in Fig. 6 (upper left panel) to look like?

(6) What will be the measurable effects, if any, of a distribution of barrier heights, $g(V_3)$? Note that we have considered a single barrier height exclusively in this paper. A distribution of barrier heights has been used extensively to model the effects of disorder on tunneling in polymers and confined molecular solids.[42–45]

(7) What effect on the ground state tunnel splitting would deuterating the CH_3 group have (that is, replace CH_3 groups with CD_3 groups)? Hint: consider how the librational frequency of the ground state changes upon deuteration [via Eq. (5)] and how this affects the overlap of the new ground state wave function through the barrier.

V. CONCLUSION

The quantum rotational dynamics for a molecular solid composed of methyl group sub-units have been discussed

using a simple parametrization of the intermolecular potential. Using this simple model we obtained a wealth of information on the dynamics of the rotor in a variety of dynamic regimes ranging from quantum tunneling to libration. The dynamics can be easily computed using standard matrix diagonalization routines, thus allowing one to visualize the time-evolution of the rotational dynamics. A simple harmonic oscillator approximation of the Hamiltonian, Eq. (3), can be used to estimate the librational transitions in the limit of infinite barrier height. Furthermore, the simple harmonic oscillator approximation can be used to illustrate the oscillatory nature of the quantum motion, appealing to our notion of the classical picture of libration. Finally, we showed that the dynamics can be measured using inelastic neutron scattering which probes the eigenvalue spectrum. The values for the tunneling and librational transitions as measured using neutron scattering are in reasonable agreement with the simple model of the rotational potential discussed here.

The simplicity of rotational tunneling, especially its ease of observation using inelastic neutron scattering, makes it an ideal example of quantum dynamics. There are numerous examples of systems that display quantum rotational dynamics as discussed here. In fact, there are over 300 systems that have been studied,[16] many of them using inelastic neutron scattering. The system presented in this paper, CH_3I, has served as one of the featured hands-on experiments for the NCNR biennial summer school on Methods and Applications of Neutron Spectroscopy.[46] Those interested in more information about the experiment can download the student handout containing instrumental and experimental details.[47] Finally, animations for rotational tunneling in the ground librational state and the first librational transition can be found on-line.[48]

ACKNOWLEDGMENTS

We are grateful to Dr. Terry Udovic for assistance using the FANS spectrometer at the NIST Center for Neutron Research (NCNR), Dr. Dan Neumann (NCNR), Dr. Samuel Trevino (U.S. Army Research Laboratory), Dr. Zema Chowdhuri (NCNR, U.MD.), Dr. Sankar Nair (NCNR), and Dr. Ronald Cappelletti (NCNR) for useful discussions. This work is based upon activities supported by the National Science Foundation under Agreement No. DMR-0086210.

APPENDIX A: MATRIX ELEMENTS OF THE METHYL ROTOR

The Hamiltonian for the rigid rotor in the threefold symmetric potential is given by Eq. (3) and reproduced here for convenience,

$$H=-\frac{\hbar^2}{2I}\frac{d^2}{d\theta^2}+\frac{V_3}{2}(1-\cos 3\theta). \tag{A1}$$

The matrix elements can be calculated using the free-rotor basis eigenfunctions,

$$\langle\theta|n\rangle_{\mathrm{FR}}=\frac{1}{\sqrt{2\pi}}\exp(in\theta)\quad (n=0,\pm1,\pm2,\pm3,\ldots). \tag{A2}$$

The Hamiltonian (A1) can be decomposed into two parts, $H_{mn}=H^0_{mn}+V_{mn}$, where the elements H^0_{mn} are related to the free-rotor energy levels as

$$H^0_{mn}=\frac{n^2\hbar^2}{2I}\delta_{mn}, \tag{A3}$$

where δ_{mn} is the Kronecker delta. This matrix element can be found via the eigenvalue equation for the free rotor Schrödinger equation,

$$-\frac{\hbar^2}{2I}\frac{d^2}{d\theta^2}\langle\theta|n\rangle_{\mathrm{FR}}=E_n\langle\theta|n\rangle_{\mathrm{FR}}, \tag{A4}$$

where the eigenfunctions are given by Eq. (A2) and the eigenfunctions are given by $E_n=Bn^2$ with $B=\hbar^2/2I=654\mu eV$. The elements of the potential matrix, V_{mn}, are found by calculating the integral,

$$V_{mn}=\int_0^{2\pi}d\theta\langle m|\theta\rangle_{\mathrm{FR}}\frac{V_3}{2}(1-\cos 3\theta)\langle\theta|n\rangle_{\mathrm{FR}}. \tag{A5}$$

Explicit calculation of (A5) and including the zero-potential energy matrix elements (A3) results in the final expression for the matrix elements of the total Hamiltonian,

$$H_{mn}=H^0_{mn}+V_{mn}, \tag{A6}$$

where

$$V_{mn}=\frac{V_3}{4}(2\delta_{mn}-\delta_{n-m+3,0}-\delta_{n+m+3,0}), \tag{A7}$$

and H^0_{mn} is given by Eq. (A3) for $n,m=0,\pm1,\pm2,\pm3,\ldots$. Standard numerical routines can be used to compute the eigenvalues and eigenvectors of Eq. (A6) to any desired accuracy.

APPENDIX B: CONVERGENCE OF THE HARMONIC APPROXIMATION TO THE LIBRATIONAL TRANSITION

The rate of convergence of the harmonic approximation to the exact first librational transition can be seen quite clearly in Fig. 5. We obtain an estimate of the convergence rate as a function of barrier height for large barriers in this appendix.

We can obtain the classical turning point about the $\theta_0=0$ equilibrium position for the ground librational state in the harmonic approximation via Taylor series expansion of the potential energy term in Eq. (3),

$$\frac{\hbar\omega_0}{2}\approx\frac{V_3}{2}\left[1-\left(1-\frac{1}{2}(3\theta_{\mathrm{tp}})^2\right)\right]. \tag{B1}$$

Next we can substitute the expression for ω_0, Eq. (5), into Eq. (B1) and arrive at the result,

$$\theta_{\mathrm{tp}}=\left(\frac{2}{9}\frac{\hbar^2}{V_3I}\right)^{1/4}. \tag{B2}$$

Table I. Evaluation of Eq. (B2) for a number of barrier heights (in units of B where $B=0.654$ meV), illustrating the slow improvement of the small-angle approximation with increasing barrier height.

V_3/B	θ_{tp} (°)	$\theta_{\mathrm{tp}}/60°$
1	62	1.0
10	35	0.58
100	20	0.33
1 000	11	0.18
10 000	6	0.1

The evaluation of θ_{tp} for a few barrier heights is shown in Table I. Because the classical turning point (that is, the maximum deviation from the equilibrium position) decreases so slowly, it is clear that the small angle approximation used in the harmonic approximation will converge slowly as well.

[a]Electronic mail: robert.dimeo@nist.gov; URL: http://www.ncnr.nist.gov/staff/dimeo

[1]Chun C. Lin and Jerome D. Swalen, ''Internal rotation and microwave spectroscopy,'' Rev. Mod. Phys. **31**, 841–891 (1959).
[2]I. F. Silvera, ''The solid molecular hydrogens in the condensed phase: Fundamentals and static properties,'' Rev. Mod. Phys. **52**, 393–452 (1980).
[3]W. Press, *Single-Particle Rotations in Molecular Crystals* (Springer Verlag, Berlin, 1981).
[4]Tung-Lin Tsai and G. Thomas, ''Analog between optical waveguide system and quantum-mechanical tunneling,'' Am. J. Phys. **44**, 636–638 (1976).
[5]E. Condon, ''Tunneling—how it all started,'' Am. J. Phys. **46**, 319–323 (1978).
[6]Jeff. D. Chalk, ''A study of barrier penetration in quantum mechanics,'' Am. J. Phys. **56**, 29–32 (1988).
[7]D. Kiang, T. Ochiai, and S. Daté, ''Tunneling through Fibonacci barriers,'' Am. J. Phys. **58**, 1200–1201 (1990).
[8]Charles W. Leming and Andrew Van Smith, ''A numerical study of quantum barrier penetration in one dimension,'' Am. J. Phys. **59**, 441–443 (1991).
[9]Oscar J. Riveros, ''Tunneling between two inequivalent potential wells,'' Am. J. Phys. **60**, 88–89 (1992).
[10]C. Julian Chen Author and Walter F. Smith, ''Introduction to scanning tunneling microscopy,'' Am. J. Phys. **62**, 573–574 (1994).
[11]H. J. Reittu, ''Fermi's golden rule and Bardeen's tunneling theory,'' Am. J. Phys. **63**, 940–944 (1995).
[12]A. Garg, ''Tunnel splittings for one-dimensional potential wells revisited,'' Am. J. Phys. **68**, 430–437 (2000).
[13]W. M. Robertson, J. Ash, and J. M. McGaugh, ''Breaking the sound barrier: Tunneling of acoustic waves through the forbidden transmission region of a one-dimensional acoustic band gap array,'' Am. J. Phys. **70**, 689–693 (2002).
[14]L. Pauling, ''The rotational motion of molecules in crystals,'' Phys. Rev. **36**, 430–443 (1930).
[15]It is interesting to note that Pauling did not refer to the tunneling motion as *rotational tunneling*. Rather he described the torsional motion (for a diatomic molecule) as one of ''oscillational states, the molecule oscillating about an equilibrium orientation and changing end for end only rarely.'' It is the rare ''end for end'' motion that is now referred to as quantum rotational tunneling. See Ref. 14, p. 434.
[16]M. Prager and A. Heidemann, ''Rotational tunneling and neutron spectroscopy: A compilation,'' Chem. Rev. **97**, 2933–2966 (1997).
[17]E. U. Condon, ''The physical pendulum in quantum mechanics,'' Phys. Rev. **31**, 891–894 (1928).
[18]T. Pradhan and A. V. Khare, ''Plane pendulum in quantum mechanics,'' Am. J. Phys. **41**, 59–66 (1973).
[19]R. Aldrovandi and P. Leal Ferreira, ''Quantum pendulum,'' Am. J. Phys. **48**, 660–664 (1980).
[20]G. P. Cook and Clyde S. Zaidins, ''The quantum point-mass pendulum,'' Am. J. Phys. **54**, 259–261 (1986).
[21]G. L. Baker, J. A. Blackburn, and H. J. T. Smith, ''The quantum pendulum: Small and large,'' Am. J. Phys. **70**, 525–531 (2002).
[22]M. Neumann and M. R. Johnson, ''Methyl group tunneling-a quantitative probe of atom-atom potentials,'' J. Chem. Phys. **107**, 1725–1731 (1997).
[23]C. J. Carlile and M. Prager, ''Rotational tunneling spectroscopy with neutrons,'' Int. J. Mod. Phys. A **7**, 3113–3151 (1993).
[24]H. W. Kroto, *Molecular Rotation Spectra* (Dover, New York, 1992), p. 56.
[25]D. F. Styer, ''The motion of wave packets through their expectation values and uncertainties,'' Am. J. Phys. **58**, 742–744 (1990).
[26]R. W. Robinett, *Quantum Mechanics: Classical Results, Modern Systems, and Visualized Examples* (Oxford U. P., New York, 1997), pp. 206–208.
[27]Reference 26, p. 59.
[28]R. W. Robinett, ''Quantum and classical probability distributions for position and momentum,'' Am. J. Phys. **63**, 823–832 (1995).
[29]Charles E. Hecht, *Statistical Thermodynamics and Kinetic Theory* (Freeman, New York, 1990), p. 115.
[30]J. Peternelj, T. Kranjc, and M. M. Pintar, ''Rotational motion of methyl groups in solids,'' Phys. Rev. B **54**, 955–961 (1996).
[31]R. K. Pathria, *Statistical Mechanics* (Butterworth-Heinemann, Oxford, 1996), 2nd ed., pp. 77–79.
[32]M. A. White and J. A. Morrison, ''Deductions about the structure of phase III from thermodynamic measurements on solid isotopic methanes,'' J. Chem. Phys. **70**, 5384–5390 (1979).
[33]K. J. Lushington and J. A. Morrison, ''Search for tunnel states in solid nitromethane,'' J. Chem. Phys. **73**, 2015–2016 (1980).
[34]S. F. Trevino, ''An observation of one-dimensional reorientation and tunnel splitting of the ground and first excited state in a low barrier system: Solid nitromethane,'' J. Chem. Phys. **71**, 1973–1974 (1979).
[35]S. F. Trevino, ''The measurement of tunnel states in solid CH_3NO_2 and CD_3NO_2,'' J. Chem. Phys. **76**, 2578–2579 (1982).
[36]G. L. Squires, *Introduction to the Theory of Thermal Neutron Scattering* (Dover, New York, 1997).
[37]A. C. Hewson, ''The temperature dependence of inelastic neutron scattering in rotational tunneling systems. I. Formulation and perturbation theory,'' J. Phys. C **15**, 3841–3853 (1982).
[38]A. Würger, ''The temperature dependence of rotational tunneling,'' Z. Phys. B: Condens. Matter **76**, 65–76 (1989).
[39]P. M. Gehring and D. A. Neumann, ''Backscattering spectroscopy at the NIST Center for Neutron Research,'' Physica B **241–243**, 64–70 (1998).
[40]J. R. D. Copley, D. A. Neumann, and W. A. Kamitakahara, ''Energy distributions of neutrons scattered from solid C_{60} by the beryllium detector method,'' Can. J. Phys. **73**, 763–771 (1995).
[41]M. Prager, J. Stanislawski, and W. Hausler, ''Inelastic incoherent neutron scattering study of the methyl rotation in various methyl halides,'' J. Chem. Phys. **86**, 2563–2575 (1987).
[42]J. Colmenero, R. Mukhopadhyay, A. Alegria, and B. Frick, ''Quantum rotational tunneling of methyl groups in polymers,'' Phys. Rev. **80**, 2350–2353 (1998).
[43]C. Gutt, B. Asmussen, I. Krasnov, W. Press, W. Langel, and R. Kahn, ''Dynamics of methane molecules in the mesopores of controlled-pore glass at low temperatures,'' Phys. Rev. B **59**, 8607–8614 (1999).
[44]A. J. Moreno, A. Alegria, J. Colmenero, and B. Frick, ''Methyl-group dynamics from tunneling to hopping in $CH_3COONa \cdot 3H_2O$: Comparison between a crystal and its glassy counterpart,'' Phys. Rev. B **65**, 134202 (2002).
[45]R. M. Dimeo and D. A. Neumann, ''Low-temperature dynamics of confined methyl iodide,'' Phys. Rev. B **63**, 014301-1–014301-9 (2001).
[46]For more details see <http://www.ncnr.nist.gov/programs/CHRNS/outreach.html>.
[47]Available via ftp at <ftp://ftp.ncnr.nist.gov/pub/staff/dimeo/hfbss_01.pdf>.
[48]<http://www.ncnr.nist.gov/staff/dimeo/rotations.html>.